Biochimica et Biophysica Acta, 767 (1984) 345–361
Elsevier

BBA 41630

NANOSECOND FLUORESCENCE FROM ISOLATED PHOTOSYNTHETIC REACTION CENTERS OF *RHODOPSEUDOMONAS SPHAEROIDES*

NEAL W.T. WOODBURY and WILLIAM W. PARSON

Department of Biochemistry SJ-70, University of Washington, Seattle, WA 98195 (USA)

(Received May 4th, 1984)

Key words: Reaction center; Fluorescence kinetics; Bacterial photosynthesis; (Rps. sphaeroides)

The time-course of fluorescence from reaction centers isolated from *Rhodopseudomonas sphaeroides* was measured using single-photon counting techniques. When electron transfer is blocked by the reduction of the electron-accepting quinones, reaction centers exhibit a relatively long-lived (delayed) fluorescence due to back reactions that regenerate the excited state (P*) from the transient radical-pair state, P^F. The delayed fluorescence can be resolved into three components, with lifetimes of 0.7, 3.2 and 11 ns at 295 K. The slowest component decays with the same time-constant as the absorbance changes due to P^F, and it depends on both temperature and magnetic fields in the same way that the absorbance changes do. The time-constants for the two faster components of delayed fluorescence are essentially independent of temperature and magnetic fields. The fluorescence also includes a very fast (prompt) component that is similar in amplitude to that obtained from unreduced reaction centers. The prompt fluorescence presumably is emitted mainly during the period before the initial charge-transfer reaction creates P^F from P*. From the amplitudes of the prompt and delayed fluorescence, we calculate an initial standard free-energy difference between P* and P^F of about 0.16 eV at 295 K, and 0.05 eV at 80 K, depending somewhat on the properties of the solvent. The multiphasic decay of the delayed fluorescence is interpreted in terms of relaxations in the free energy of P^F with time, totalling about 0.05 eV at 295 K, possibly resulting from nuclear movements in the electron-carriers or the protein.

Introduction

When reaction centers from the photosynthetic bacterium *Rhodopseudomonas sphaeroides* absorb light, a bacteriochlorophyll dimer (P) is oxidized, giving rise to a transient radical-pair state (P^+I^- or P^F) within 7 ps [1–7]. This state decays in about 200 ps to the state P^+Q^-, where Q is a ubiquinone [2,3,5,8]. P^F appears to be a mixture of the states P^+BChl^- and P^+BPh^-, where BChl and BPh are bacteriochlorophyll and bacteriopheophytin [9–11]. If electron transfer to Q is blocked by the chemical reduction of Q, or by extracting Q from the reaction centers, P^F decays by several pathways [8,11–15]. Charge recombination apparently can occur directly to the ground state (P); spin rephasing also can occur, giving rise to a radical-pair state with triplet character ($^3[P^+I^-]$) that decays to a longer-liver triplet state (P^R) [11–13,15]. Alternatively, back electron transfer can regenerate P*, which can then decay to the ground state nonradiatively or by fluorescing [11,15–21]. The 'delayed' fluorescence that is emitted during the lifetime of P^F provides a useful probe of the kinetic and thermodynamic properties of the metastable state.

The decay of the absorption changes associated

Abbreviations: BChl, bacteriochlorophyll; BPh, bacteriopheophytin.

with P^F in reaction centers with Q reduced or extracted appears to be well described by a single exponential with a lifetime of 10–15 ns at room temperature [2,13,15,19]. The decay constant decreases with decreasing temperature and at 80 K is about half as great as at 295 K. The quantum yield of state P^R increases from approx. 0.1 to about 0.5 with the same drop in temperature. Weak magnetic fields slow the decay of P^F and decrease the quantum yield of P^R by interfering with the spin rephasing process $^1[P^+I^-] \rightleftharpoons {}^3[P^+I^-]$, though the details of this process are still uncertain [15,20–24].

In contrast, most measurements of delayed fluorescence have given lifetimes of 4–6 ns, i.e., only about half as long as the lifetime of state P^F [15,17,18,25,26]. However, Van Bochoven et al. [27] found the delayed fluorescence from chromatophores to be composed of two components, a long-lived component with roughly the same lifetime as P^F and a shorter component with a lifetime between 3 and 5 ns. The dependence of the fluorescence decay kinetics on temperature and magnetic fields has not been measured with high precision, but the average lifetime of the delayed fluorescence appears to be relatively insensitive to temperature in both chromatophores [27] and reaction centers [15]. Weak magnetic fields cause a small increase in the average lifetime of delayed fluorescence from chromatophores [27], but this effect has not been detected in isolated reaction centers [15]. Magnetic fields cause a small increase in the integrated yield of delayed fluorescence in both systems [15,27–29].

In the present study, we examined the decay kinetics of the delayed fluorescence from isolated reaction centers more closely, using the high time-resolution obtainable by single-photon counting. We compared the fluorescence kinetics to the decay kinetics that have been described previously for the absorbance changes associated with P^F over a wide range of temperatures and in the presence and absence of magnetic fields. One aim of the study was to resolve the apparent inconsistencies noted above.

Measurements of delayed fluorescence can be used to estimate the differences in standard free energy and enthalpy between P* and P^F. From the temperature dependence of the delayed fluorescence yield of *Chromatium vinosum* reaction centers, Shuvalov and Klimov calculated that P^F lies 0.12 eV below P* in enthalpy [9]. Van Grondelle et al. similarly calculated an apparent enthalpy difference of approx. 0.14 eV in various species of chromatophores [16], but this was later reevaluated to be 0.05 eV by Rademaker and Hoff, who took into account the fact that the fluorescence from chromatophores is emitted mainly by the antenna BChl rather than by P* [24,30–32]. Godik et al. [25] calculated an apparent enthalpy difference of 0.09 eV based on the fluorescence yield in *Rhodospirillum rubrum* chromatophores, but their calculation did not consider the temperature dependence of the distribution of excitations between the reaction center and the antenna.

The thermodynamic parameters that have been derived from the integrated yield of delayed fluorescence are of questionable significance, because they could be influenced by a temperature dependence of the fluorescence decay kinetics. By measuring the initial amplitude of the delayed fluorescence from *Rhodopseudomonas sphaeroides* reation centers, Schenck et al. [15] obtained a free energy difference of 0.18 eV between P* and P^F at 295 K *. However, Schenck et al. [15] were not able to resolve the complicated decay kinetics of the fluorescence completely, and thus could have underestimated the initial amplitudes.

The calculations of the enthalpy gap between P* and P^F that have been based on the temperature dependence of the delayed fluorescence are subject to additional uncertainties. For reasons that are not understood, the yield and initial amplitude of the delayed fluorescence from isolated reaction centers of *Rps. sphaeroides* increase with decreasing temperature from 270 down to about 200 K [15,33]. This is contrary to what one would expect for any simple model, if P^F lies below P* in energy. Clayton [33] reported that the yield of the total luminescence was essentially independent of temperature below 200 K, but Schenck et al. [15] found that the delayed fluorescence decreased in amplitude and yield below this point while the prompt fluorescence remained constant.

In this report, we calculate the free-energy gap

* The free energy value of 0.25 eV reported by Schenck et al. [15] includes an arithmetic error; the value given here is obtained by reevaluating the data in their Fig. 7.

between P^* and P^F in *Rps. sphaeroides* reaction centers from measurements of the initial amplitude of the delayed fluorescence. The calculations involve a comparison with the fluorescence from a standard with a known quantum yield [15,26]. Again, the improved time resolution made possible by single-photon counting should help to resolve some of the uncertainties that have remained from previous studies. Results are presented for temperatures from 80 to 295 K, for the presence and absence of weak magnetic fields, and for variations in the properties of the solvent.

A preliminary report of this work has been presented [34].

Methods

Reaction centers were prepared from *Rps. sphaeroides* strain R26 as described [15], dialysed against 50 mM Tris (pH 8.0)/0.05% triton X-100, and stored frozen at −20°C at high concentration (absorbance$_{800} \geqslant 10$). At the time of the measurement, the reaction centers were diluted with 10 or 50 mM Tris (pH 8.0) containing 0–0.05% Triton X-100 and glycerol as specified below. When pH was varied, Tris was used between pH 7 and 9, glycine between pH 9 and 10.6, and phosphate between pH 6 and 7. Reduction of Q was accomplished by addition of approx. 1 mg of sodium dithionite to 2.5 ml of sample. Increasing the buffer concentration from 10 to 50 mM did not affect the fluorescence signal, indicating that any pH change caused by the dithionite was inconsequential.

The sample was excited at 600 nm with a vertically polarized 25 ps pulse from a cavity-dumped rhodamine dye laser (Spectra Physics model 375), which was synchronously pumped by an argon ion laser (model 171). The pulse repetition rate was 0.8 MHz. The sample was held in a cryostat (Janus, Inc.) that allowed accurate temperature control by flowing cold nitrogen over the sample holder and by electrical heating of the holder. Cuvettes were made of thick-walled square quartz tubing (0.5 inch external width), fitted with a septum to exclude oxygen. Excitation at a right angle to detection was used to avoid an artifact due to fluorescence or scattered excitation light from quartz directly in the path of the excitation beam. The aluminum cuvette holder was made with three windows (entrance of excitation light, exit of excitation and fluorescence detection) so as to minimize the detection of fluorescence from the quartz. The excitation light intensity was monitored with a photodiode, integrating preamplifier and chart recorder, and was controlled with calibrated neutral density filters. The light intensity was low enough so that the fluorescence signal was linear in the intensity in all cases; actual intensities are given in the figure legends.

Fluorescence was detected by an S1 photomultiplier (Hamamatsu R632) that was equipped with a 920 nm interference filter (20 nm bandpass) and cooled with solid CO_2. The fluorescence was collimated by a lens close to the sample and focused by a second lens on the center of the photocathode, which was approx. 0.8 m from the sample. A 600 G magnetic field was produced by a home-made electromagnet placed so that the field was at 45° to the excitation and detection axes.

Fluorescence emission spectra were measured using the same single-photon counting apparatus, after replacing the interference filter by a monochromator and a Corning 2600 infrared-transmitting filter. The spectra were obtained using a concentration of reaction centers (0.7 μM) that gave an absorbance$_{800}$ of approx. 0.2. The absorbance at 900 nm was about 0.05, so that self-absorption of the fluorescence was insignificant. The wavelength dependence of the photomultiplier and monochromator was determined by measuring the emission spectrum of a standard (black body) lamp [35], and the emission spectra shown are corrected for this effect. The monochromator greatly decreased the photon counting rate, and therefore was not used routinely. From the fluorescence emission spectra, we calculated that the apparatus detected the same fraction of the total fluorescence at all temperatures to within ±7% of the mean. The fraction of the fluorescence that is transmitted by the interference filter depends slightly on the temperature because the emission bands sharpen and shift to longer wavelengths with decreasing temperature. Since this effect was minor, no correction to the data was made.

The single-photon counting electronics [36] consisted of an Ortec model 4890 preamplifier, model 934 constant fraction discriminator, and model

457 time-to-amplitude converter, followed by a Tracor Northern TN1705 pulse height analyzer. 512 channels of data (80 ps per channel) were collected.

Absorption spectra were measured with a GCA-McPherson spectrophotometer equipped with a home-built cryostat.

Results

Fig. 1 shows the time-course of fluorescence from reaction centers with Q in the reduced and unreduced states, as measured with the single-photon counting apparatus. The width of the signal obtained with the unreduced sample is about 1 ns; this reflects the response time of the apparatus.

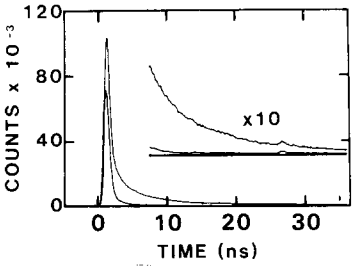

Fig. 1. The time-course of fluorescence from reduced (upper curves) and unreduced (lower curves) reaction centers at 295 K. Samples were in 75% glycerol as described in Methods and had an absorbance at 600 nm of 0.5 (reaction center concentration, 7.3 μM). The data for unreduced reaction centers were collected in two sets, totaling 5550 s, with a counting rate of approx. 300 counts per s. The incident light intensity was approx. 0.05 $mW \cdot cm^{-2}$ ($1.5 \cdot 10^{14}$ photons per s per cm^2). This photon density is calculated to give a steady state P^+Q^- level of approx. 1% of the total P, on the assumption that P^+Q^- decays with a time constant of 1 s, and less if the decay is faster. The light intensity during the measurement of reduced reaction centers was approx. 0.2 $mW \cdot cm^{-2}$. (A higher light intensity can be used after the reduction of Q, because of the short lifetime of P^F and P^R.) The counting rate was approx. 4000 counts per s (0.5% of the laser frequency), which was low enough that double-photon events would be infrequent. Data were collected for 2000 s, alternating every 200 s between the presence and absence of a 600 G magnetic field (thus resulting in 1000 s of data collected under each condition stored in two separate channels). The trace shown was obtained in the absence of a magnetic field. The data for reduced reaction centers are scaled vertically to correct for the different light intensity and counting time. The small peaks near 14 and 26 ns in the expanded signals result from secondary laser pulses that are not completely suppressed by the acousto-optic cavity dumper in the dye laser. These do not affect the results, because the deconvolution procedure takes them into account.

(The actual fluorescence lifetime of unreduced reaction centers is probably about 7 ps [1–7].)

The measurements of reduced reaction centers were deconvoluted by using the signal from the same sample of reaction centers in the unreduced state as the excitation profile, and were analyzed assuming two, three, or four kinetic components. In each case one of the components was assumed to be 'prompt' fluorescence with the same profile as the excitation, but with an adjustable yield. The contribution of the prompt fluorescence to the signal at time t thus was taken to be $\alpha F_M(t)$ where $F_M(t)$ is the signal from unreduced reaction centers and α is a dimensionless relative yield. A relative yield of 1.0 corresponds to an absolute yield of approx. $4 \cdot 10^{-4}$ [1]. The contributions from delayed fluorescence were calculated by convoluting $F_M(t)$ with a sum of one, two or three exponential decay functions, $B_i e^{-t/\tau_i}$. The amplitude factors B_i have units of s^{-1}, but are automatically scaled, so that the product $B_i\tau_i$ gives the integrated yield of fluorescence in component i, relative to the fluorescence yield from unreduced reaction centers. Except for the use of a larger number of exponential components, this analysis is basically the same as that described previously [15].

An unreduced sample was used to obtain the excitation profile because we were unable to find a sufficiently short-lived fluorescence standard at the detection wavelength (920 nm). Scattered light from the excitation laser itself is unsatisfactory, because it is difficult to insure that it follows exactly the same optical path to the photomultiplier, and because its wavelength (600 nm) is too far from the detection wavelength; the phase shift introduced by the photomultiplier is a function of the wavelength.

The curve fitting was performed with statistical weighting essentially as described [37]. Thus the reduced Chi square value was calculated as:

$$\chi^2 = \frac{1}{N-n} \sum_{i=1}^{N} \frac{(y_i - c_i)^2}{y_i'}$$

where y_i and c_i are the observed and calculated number of counts at time point i, y_i' is a smoothed value of y_i obtained by a three point averaging, N is the total number of points, and n is the number

of free parameters. The fitting procedure minimizes χ^2. Fig. 2 shows the residual $y_i - c_i$ obtained by subtracting several different calculated curves from an observed signal. The residual has been divided by the calculated standard deviation of the observed signal at each point ($\sqrt{y_i'}$), so that the vertical scale gives the error in standard deviations from the observed signal. If the errors are due simply to random statistical fluctuations in the signal, the scaled residuals should lie mainly (67%) within ± 1 standard deviation from zero and should not vary systematically with time. The residuals resulting from fits assuming one, two or three exponential components are shown. Only fits using three or more exponential components are satisfactory (Fig. 2c); the curves calculated with either one or two exponentials deviate systematically from the observed signal (Fig. 2a and 2b). Similar results were obtained consistently with two independent preparations of reaction centers, and three-exponential fits therefore were used to analyze all of the data. There are eight free parameters in these fits: three exponential decay times (τ_i) and corresponding amplitudes (B_i), a prompt fluorescence yield (α), and a phase-shift parameter that allows correction for small shifts in the relative time of the laser pulse between the measurement of the excitation profile and that of the signal. Such shifts can arise from slight instabilities in the electronics over long periods of time. The phase shift was included in the curve-fitting program as a free parameter, essentially as described by Grinwald [38]. Altough the shift generally was less than one time-point (0.08 ns), correcting for it significantly improved the reproducibility of determining the other parameters.

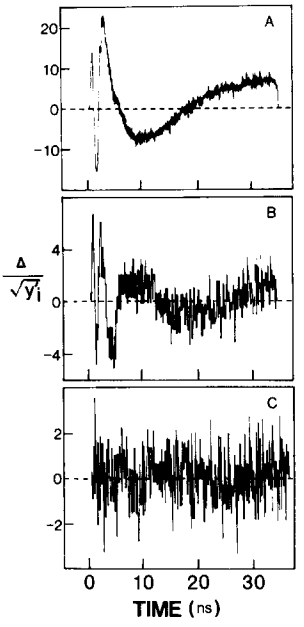

Fig. 2. Curve-fitting residuals derived by dividing the difference between the calculated and observed signals by the square root of the number of counts at each point. The divisor was smoothed as explained in the text. The vertical axis gives the error in standard deviations from the observed signal. (A) Fit assuming two components: one with the same profile as the excitation pulse (prompt fluorescence) and one with an exponential decay (delayed fluorescence); $\chi^2 = 49$. (B) Fit assuming three components: prompt fluorescence and two exponential components of delayed fluorescence; $\chi^2 = 2.9$. (C) Fit assuming four components: prompt fluorescence and three exponential components of delayed fluorescence; $\chi^2 = 1.2$. The fits were obtained as outlined in the text using the data shown in Fig. 1.

One might ask whether delayed fluorescence due to the transient presence of the state P^F in unreduced reaction centers invalidates our use of the fluorescence from unreduced reaction centers as an excitation profile. We considered this point by assuming that delayed fluorescence from P^F in unreduced reaction centers occurs with the same initial amplitude as that calculated for the delayed fluorescence after reduction of Q, but decays with a time constant of 200 ps. The excitation profile can be corrected by removing the calculated 200 ps component after deconvolution. The signal from the reduced reaction centers is then refit; a new amplitude is obtained; and the iteration is continued until convergence. The result of the calculation is that about 15% of the fluorescence from unreduced reaction centers is due to delayed fluorescence. When this delayed fluorescence is removed from the excitation profile, the calculated relative amplitude of the fast component of the delayed fluorescence increases by about 50% at both room temperature and at 80 K; the calculated amplitudes of the other delayed fluorescence components and the prompt fluorescence yield increase by about 20% (relative to the excitation pulse). This results in only a 0.006 eV decrease in the calculated free-energy gap between P* and P^F at 295 K (see below). It has no qualitative effect on the temperature dependence of any measured components. For these reasons and because it

TABLE I

COMPONENTS OF THE FLUORESCENCE FROM REDUCED REACTION CENTERS AT 295 K

Sample	Field [c]	Total yield [d]	α	Amplitudes (ns^{-1})			Time constants (ns)			χ^2	ΔG^e (eV)
				B_1	B_2	B_3	τ_1	τ_2	τ_3		
Glycerol [a]	–	2.36 ± 0.12	1.26 ± 0.06	0.28 ± 0.09	0.12 ± 0.02	0.051 ± 0.005	0.67 ± 0.12	3.2 ± 0.2	10.6 ± 0.4	1.3	0.157 ± 0.006
	+	2.40 ± 0.12	1.25 ± 0.06	0.30 ± 0.11	0.12 ± 0.02	0.047 ± 0.006	0.66 ± 0.15	3.4 ± 0.3	12.3 ± 0.5	1.2	0.156 ± 0.006
Aqueous [b]	–	2.20 ± 0.24	1.21 ± 0.12	0.14 ± 0.02	0.10 ± 0.02	0.049 ± 0.007	0.98 ± 0.08	3.8 ± 0.3	10.2 ± 0.3	1.2	0.168 ± 0.004
	+	2.28 ± 0.29	1.22 ± 0.13	0.14 ± 0.03	0.10 ± 0.01	0.046 ± 0.012	1.02 ± 0.05	4.1 ± 0.4	11.6 ± 0.7	1.1	0.169 ± 0.006

[a] 25% (w/w) Tris/Triton buffer (50 mM Tris/0.02% Triton X-100, pH 8.0) and 75% (w/w) glycerol, 7.3 μM reaction centers. Average of five independent measurements.

[b] Tris/Triton buffer. 7.3 μM reaction centers. Averages of four independent measurements.

[c] + means 600 G external field; – means no applied field other than the small residual field from the electromagnet.

[d] Total fluorescence yield relative to the fluorescence yield of the same sample in the unreduced state.

[e] Free-energy difference calculated for the reaction $P_1^F \rightarrow P^*$; P_1^F is the earliest form of P^F that is resolved by the measurement.

involves questionable assumptions about the nature of fluorescence in unreduced reaction centers, the corrected excitation pulse was not used for the analysis of any of the data presented.

Table I presents the results of measurements made on reaction centers at 295 K. Five pairs of measurements were made with relatively concentrated suspensions of reaction centers (7.3 μM) in 75% glycerol and 25% Tris/Triton buffer in the presence and absence of a magnetic field. Four pairs were made with similar suspensions in the absence of glycerol. The table gives the means of the fluorescence parameters obtained in each series, with the standard deviations of the individual measurements about the means. In 75% glycerol, the total fluorescence yield increases by about a factor of 2.4 upon reduction of the quinone. The bulk of this increase is due to the appearance of delayed fluorescence, although the yield of prompt fluorescence also increases by about 25% (α is about 1.25). the delayed fluorescence decays in three components, with lifetimes of 0.67, 3.2 and 10.6 ns. The 0.67 ns component has about twice the initial amplitude of the 3.2 ns component, which has about twice the initial amplitude of the 10.6 ns component. The presence of a 600 G magnetic field causes the total yield of fluorescence in reduced reaction centers to increase only marginally *. There is, however, a significant increase in the lifetime of the longest component of delayed fluorescence from 10.6 to 12.3 ns. No other parameter changes significantly in the presence of the magnetic field. All of the parameters were reproducible to within $\pm 20\%$ of the mean in measurements with different reaction center samples, except for the initial amplitude and lifetime of the fastest component of delayed fluorescence, which varied by as much as $\pm 30\%$ of the mean between measurements. The results for samples in aqueous buffers were similar except that the fastest component of delayed fluorescence had a lower initial amplitude and a slower decay. The decay of the intermediate component of delayed fluorescence also was somewhat slower in the aqueous samples than in the presence of 75% glycerol.

A series of individual measurements of fluorescence was made under a wider range of conditions.

* The effects of the magnetic field on the total yield of fluorescence and on τ_3 are both more significant statistically if one considers pairs of measurements made on the same occasion with and without the field. The standard deviations of the averaged data shown in Table I include day-to-day variations in the sample and the apparatus.

TABLE II

COMPONENTS OF THE FLUORESCENCE FROM REDUCED REACTION CENTERS AT 295 K

[RC] [a] (μM)	Triton (%)	Total yield [b]	α	Amplitudes (ns^{-1})			Time constants (ns)			ΔG [c] (eV)
				B_1	B_2	B_3	τ_1	τ_2	τ_3	
0.60	0.05	2.7	1.4	0.30	0.13	0.06	0.7	3.3	10.6	0.154
0.76	0.015	3.4	1.6	0.36	0.16	0.08	0.7	3.5	10.9	0.149
0.73	0.007	3.7	1.8	0.37	0.19	0.09	0.8	3.6	10.9	0.147
0.66	0.002	4.0	1.9	0.36	0.19	0.10	1.0	3.8	11.3	0.147
0.88	0.0004	3.8	1.6	0.38	0.21	0.10	0.9	3.5	11.4	0.146
4.20	0.003	2.7	1.5	0.23	0.19	0.05	0.9	2.8	10.0	0.155
2.10	0.0015	3.6	1.7	0.46	0.29	0.10	0.6	2.7	10.2	0.150
0.54	0.0004	4.5	1.7	0.65	0.33	0.14	0.6	2.9	10.6	0.133
0.23	0.0002	4.8	1.6	0.96	0.39	0.15	0.5	2.0	10.8	0.126
0.13	0.00009	5.5	1.8	1.10	0.42	0.17	0.6	3.0	10.5	0.123
0.07	0.00005	4.5	1.5	0.92	0.34	0.14	0.7	3.1	10.7	0.128

[a] Reaction center concentration. All data represent single measurements in the absence of an applied field. The conditions were as in Table I, footnote a, except that for the sample with 0.05% triton, the ionic strength was increased from 8 to 27 mM.

[b] Total fluorescence yield, relative to the fluorescence yield of the same sample in the unreduced state.

[c] Free-energy difference for the reaction $P^F \rightarrow P^*$.

The decay time constants for the three components of the delayed fluorescence do not depend greatly on the detergent concentration, reaction center concentration, pH or ionic strength. However, variations in some of these parameters do result in changes in the initial amplitudes of the three components (Table II). In the presence of glycerol, decreasing the detergent concentration increases the initial amplitudes of all three components of the delayed fluorescence (and thus the total fluorescence yield) and has a similar but smaller effect on the prompt fluorescence yield. Similar effects are obtained by diluting the reaction centers and detergent together so as to maintain a constant ratio between their concentrations. A systematic study of these effects is difficult, because the reaction centers are added with an unknown amount of bound detergent. However, the apparent quantum yield of fluorescence from unreduced reaction centers was independent of the reaction center concentration over the range studies here, so the increase in the relative yield of delayed fluorescence at low concentrations of reaction centers and detergent was probably not due to changes in self-absorption. The effect of the detergent concentration is smaller (and probably insignificant) in the absence of glycerol (data not shown). Variations in the ionic strength (between 8 and 105 mM) at constant detergent concentration have little or no effect on the fluorescence (not more than 20%). Increasing the pH over the range 6–10.6 causes an increase in the amplitudes of the two faster components of the delayed fluorescence by about a factor of 2.

The fluorescence components were studied as functions of temperature between 80 and 300 K. Fig. 3 shows the total fluorescence yields from reduced and unreduced reaction centers, and the yield of the prompt component of fluorescence from reduced reaction centers. All of the yields are expressed relative to the total fluorescence yield from the same sample of reaction centers in the unreduced state at room temperature. The total yield of fluorescence from reduced reaction centers is shown for three different concentrations of reaction centers (0.15, 0.73 and 7.3 μM), all with the same ratio of added detergent to reaction center concentration (Fig. 3A, open symbols). The prompt fluorescence yield from reduced reaction centers

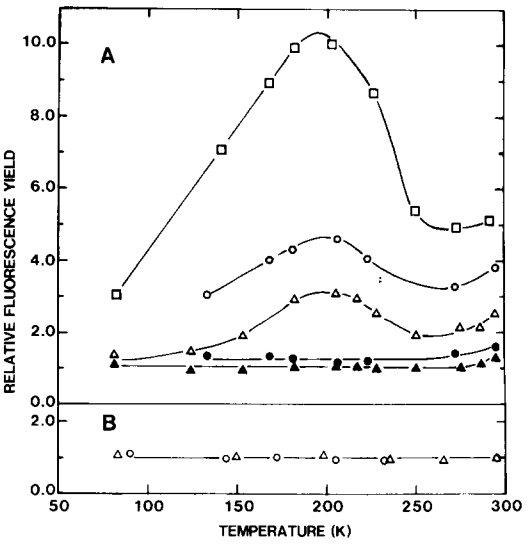

Fig. 3. Fluorescence yield as a function of temperature. All yields are given relative to the fluorescence yield of unreduced reaction centers at 295 K. (A) Total fluorescence (open symbols) and prompt fluorescence (closed symbols) from reduced reaction centers. (△———△), 7.3 μM reaction centers with 0.005% added Triton. (○———○), 0.73 μM reaction centers with 0.0005% added triton. (□———□), 0.15 μM reaction centers with 0.0001% added triton. For the lowest concentration, the light intensity was increased by a factor of approx. 2 over that given in Fig. 1. For the other samples the conditions were as in Fig. 1. The prompt fluorescence yield (α) was obtained by deconvolution, as described in the text. The total fluorescence yield was obtained from the same measurements by integration or (with equivalent results) by summing the calculated prompt fluorescence yield and the products of the initial amplitudes and decay time constants of the three components of the delayed fluorescence. (B) Fluorescence yield from unreduced reaction centers. (△———△), 7.3 μM reaction centers with 0.005% added triton. (○———○), 0.73 μM reaction centers with 0.0005% added triton.

(Fig. 3A, closed symbols) and the fluorescence yield from unreduced reaction centers (Fig. 3B) are shown for the two higher concentrations of reaction centers. (The lowest reaction center concentration gave too little fluorescence for these quantities to be measured accurately.) In agreement with the observations by Schenck et al. [15], the total fluorescence from reduced reaction centers drops as the temperature is lowered to about 250 K, increases to a maximum near 200 K, and then decreases substantially by 80 K. The increase in fluorescence upon cooling to 200 K becomes more dramatic as the detergent (and reaction center)

concentration is lowered. The yield of prompt fluorescence from reduced reaction centers decreases slightly with temperature down to about 270 K and then becomes essentially constant. The fluorescence yield from unreduced reaction centers also is relatively insensitive to temperature, and its behavior is not altered significantly by a 10-fold reduction in reaction center (and detergent) concentration (Fig. 3B). This indicates that the complex temperature dependence seen in reduced reaction centers is probably not an artifactual effect of changes in self-absorption with decreasing temperature (see also Methods).

A detailed study of delayed fluorescence was done using 7.3 μM reaction centers (0.005% Triton). The high reaction center concentration made accurate measurements of the fluorescence possible at a number of temperatures in the presence and absence of a magnetic field during a single session. a similar study was done with a more dilute sample of reaction centers, but these measurements were made at fewer temperature points and only in the absence of the magnetic field. Data from the high-concentration study are shown in Figs. 4 and 5.

The decay rate constants of the fast and intermediate components of delayed fluorescence do not vary appreciably with temperature (Fig. 4). The rate constant for the slowest component, however, decreases by about a factor of two with decreasing temperature between 295 and 200 K, and continues to decrease slightly below 200 K. The temperature dependence of the slow component is essentially identical to that of the absorbance changes associated with the state P^F [15]. Magnetic fields retard the decay of the slow component at all temperatures, as they do the decay of P^F [15].

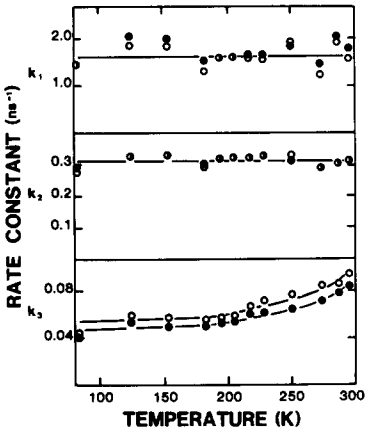

Fig. 4. The decay rate constants (k_1, k_2, k_3) of the three components of delayed fluorescence as functions of temperature. (These are the reciprocals of the time-decay constants.) (○——○), no magnetic field. (●——●), 600 G magnetic field. Conditions as in Fig. 1. Each point in Figs. 4 and 5 represents the average of two independent measurements except for the two lowest temperatures, which are single measurements.

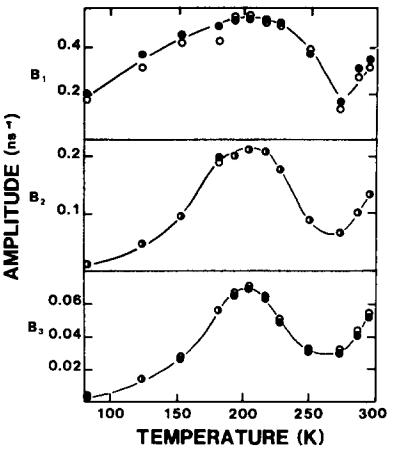

Fig. 5. The initial amplitudes of the three components of delayed fluorescence (B_1, B_2, B_3) as functions of temperature. The amplitudes have units of s^{-1}, but are scaled dimensionlessly relative to the total fluorescence yield from unreduced reaction centers at 295 K. (○——○), no magnetic field. (●——●), 600 G magnetic field. Conditions as in Fig. 1.

Fig. 5 shows the initial amplitudes of the three components of the delayed fluorescence as functions of temperature. The amplitudes all decrease with decreasing temperature down to about 270 K, increase to a maximum near 200 K, and then decrease. The amplitudes of the longest-lived and intermediate components (B_3 and B_2) fall to nearly zero by 80 K; that of the shortest-lived component (B_1) also decreases, but not as sharply. The changes in the amplitudes of the delayed fluorescence components account for most of the temperature dependence of the total fluorescence yield (Fig. 3). When the reaction centers were diluted 10-fold by buffer containing no detergent, the temperature dependence of the amplitudes and decay constants was qualitatively similar to that seen at the higher

reaction center/detergent concentration. However, the decrease in the B_2 and B_3 between 295 and 270 K was not as pronounced, and was absent entirely in B_1 (data not shown).

To determine the effect of temperature on the radiative properties of P*, we measured absorption and emission spectra of reaction centers as a function of temperature. The long-wavelength absorption band of P sharpens and shifts from about 869 nm at 295 K to about 888 nm at 150 K (Fig. 7). The spectrum of the longest-lived component of delayed fluorescence was obtained by integrating photons collected between 10 and 38.5 ns after the beginning of the excitation function. The maximum in this spectrum also shifts with decreasing temperature, from 913 nm at 295 K to 925 nm at 80 K (Figs. 6 and 7). The spectrum of the long-lived component was compared to that of the fluorescence emitted between 0 and 2 ns, which is composed primarily of prompt fluorescence (Fig. 6). The 0–2 ns spectrum contains a small peak near 800 nm, in addition to the main peak near 915 nm. Clayton [33] and Slooten [39] have described a similar short-wavelength fluorescence previously, and have ascribed it to impurities in the reaction center preparation.

The short-wavelength fluorescence could explain the apparent discrepancy between our observations on the temperature dependence of the fluorescence yield (Figs. 3 and 5) and the results described by Clayton [33]. Clayton reported that, with reaction centers in glycerol, there was no decrease in the yield of 920 nm fluorescence between 200 and 80 K. This is possibly because the short-wavelength fluorescence increased substantially over the same temperature range [33]. The tail of the short-wavelength fluorescence may have extended into the 920 nm fluorescence, causing the total fluorescence at 920 nm to remain fairly constant as the temperature was lowered. In dried films of reaction centers, where little short-wavelength fluorescence was observed, Clayton did see

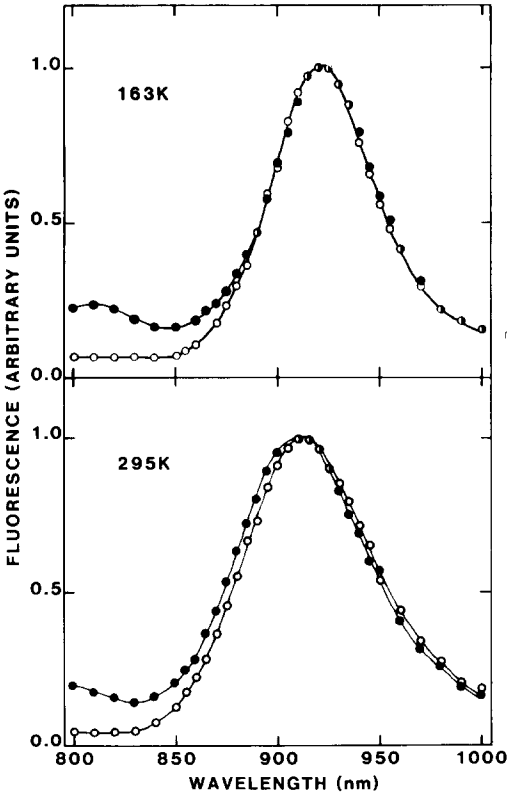

Fig. 6. Spectra of fluorescence from reduced reaction centers (0.7 μM) in 0.05% added Triton and 75% glycerol at 295 and 160 K. Closed symbols represent photons counted between 0 and 2 ns after the beginning of the excitation function; open symbols, photons counted between 10 and 38.5 ns (see time scale, Fig. 1). The band-pass of the monochromator was 7 nm. The light intensity was approx. 3 mW·cm^{-2} ($9 \cdot 10^{15}$ photons per cm^2 per s).

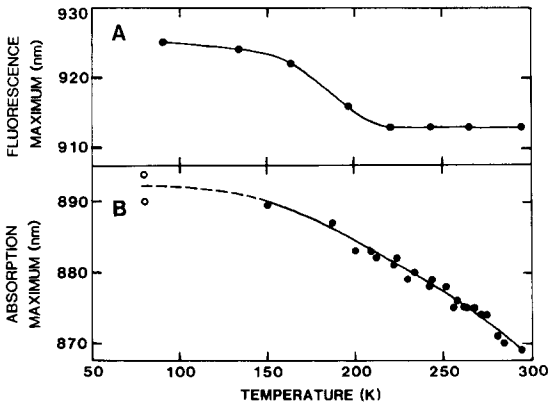

Fig. 7. (A) Wavelength of maximum fluorescence as a function of temperature. Maxima determined from spectra like those in Fig. 6. The measurement at 90 K represents the total fluorescence; those at higher temperatures, the fluorescence between 10 and 38.5 ns after the beginning of the excitation function. (B) Wavelength of maximum absorption as a function of temperature. Closed symbols indicate our measurements; open symbols, data from Ref. 55 (upper point) and Ref. 56 (lower point).

a substantial decrease in the 920 nm fluorescence between 200 and 80 K, though not as great as the decrease observed here. As shown in Fig. 3, the amount of decrease in the 920 nm fluorescence between 200 and 80 K depends on the conditions of the sample.

There is a small difference between the 0–2 ns and 10–38.5 ns spectra at room temperature. The longer-lived fluorescence peaks at about 913 nm; the short-time fluorescence, at about 911 nm. This could be due to contamination of the long-wavelength fluorescence by the tail of the short-wavelength fluorescence in the 0–2 ns spectra. As the temperature is decreased, the difference between the maxima decreases and disappears by 160 K (Fig. 6). At 133 K, the longer-lived fluorescence may be shifted slightly (about 2 nm) to the blue of the 0–2 ns fluorescence (data not shown).

Discussion

The free energy gap between P and the initial form of P^F*

It seems reasonable to assume that all of the delayed fluorescence at 920 nm from reduced reaction centers is emitted by P*, and results from charge recombination in the state P^F. The delayed fluorescence is unlikely to come from impurities in the preparation, or from grossly damaged reaction centers, because it is not seen until electron transfer is blocked between I^- and Q.

Because the initial formation of P^F is much faster than the decay of the delayed fluorescence, an apparent equilibrium constant for the reaction $P^F \rightleftharpoons P^*$ can be calculated from the expression [15,40]:

$$K = (F_D(0)\Phi_f)/k_f \qquad (1)$$

Here $F_D(0)$ is the initial amplitude of delayed fluorescence (the sum of the initial amplitudes of the three decay components) relative to the fluorescence yield from unreduced reaction centers, Φ_f is the quantum yield of fluorescence from unreduced reaction centers, and k_f is the reciprocal of the natural radiative lifetime of P*. By considering $F_D(0)$, we focus on the form of P^F that is present at the earliest resolvable times after the excitation. As discussed below, P^F probably relaxes from this form (P_1^F) to forms with lower free energies.

A value of $8 \cdot 10^7\ s^{-1}$ was calculated for k_f from the absorption spectrum at 295 K by the Strickler-Berg equation [41], in agreement with previous calculations [15]; $9 \cdot 10^7\ s^{-1}$ was obtained from the fluorescence emission spectrum by the treatment of Ross [42] as developed by Arata and Nishimura [43]. The value of k_f is essentially independent of temperature ($\pm 6\%$ of the mean), at least down to 160 K (data not shown). Using $k_f = 8.5 \cdot 10^7\ s^{-1}$ and $\Phi_f = 4 \cdot 10^{-4}$ (Ref. 1), the apparent equilibrium constant for the conversion of the initial form of P^F back to P* is calculated to be about $2.5 \cdot 10^{-3}$ for 7.3 μM reaction centers in 0.005% triton and 75% glycerol at room temperature. This is equivalent to a standard free energy change (ΔG) of about 0.157 eV (Table I). Slightly higher values of ΔG were obtained in the absence of glycerol (Table I), and somewhat lower values were obtained when the concentration of detergent (or detergent and reaction centers) was decreased (Table II). Lowering the pH to 6 caused an increase in ΔG of about 0.01 eV (data not shown). Increasing the pH to 10.6 or varying the ionic strength had no significant effect on ΔG. Thus the free energies observed under a variety of conditions ranged from 0.12 to 0.17 eV.

The temperature dependence of the calculated free energy difference between P* and the initial form of P^F is given in Fig. 8 for two reaction center/detergent concentrations. As reflected in

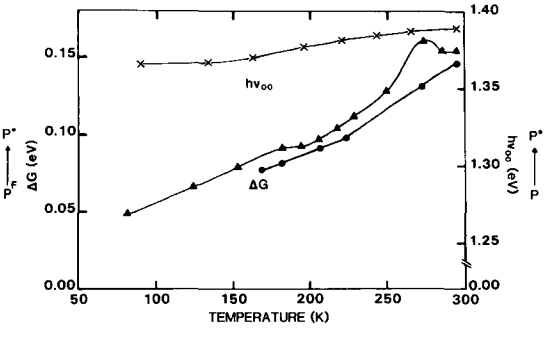

Fig. 8. Free energy difference between P* and P^F as a function of temperature, with 7.3 μM reaction centers in 0.005% triton (▲——▲), or 0.73 μM reaction centers in 0.0005% triton (●——●). (×——×), The 0-0 transition energy of P* calculated from the average energy of the absorption and emission maxima (Fig. 7).

the initial amplitude of the delayed fluorescence (Fig. 5), ΔG has a nonlinear dependence on temperature in the region between 295 and 180 K, and then decreases in a roughly linear fashion as the temperature is decreased below 180 K. Judging from the linear region between 80 and 180 K, the equilibrium between P* and P^F appears to be dominated by an entropic process. Using the expression $\Delta G = \Delta H - T\Delta S$, one obtains $\Delta H \approx 0.015$ eV and $\Delta S \approx -6.5 \cdot 10^{-4}$ eV/K for the higher of the two reaction center/detergent concentrations. Above 180 K, additional processes occur or there are changes in ΔH or ΔS causing the relationship between ΔG and temperature to deviate significantly from linearity. The extent of this deviation appears to depend on the detergent concentration (Fig. 8).

In principle, the nonlinearities in the dependence of ΔG on temperature could arise from changes in the energy of P* with decreasing temperature. To test this possibility, the 0-0 transition energy of P* was estimated from the fluorescence and absorption spectra by averaging the energies of the absorption and emission maxima at each temperature. The 0-0 transition energy decreases with temperature, as reported previously [44], but this change is not sufficient to account for the nonlinear temperature dependence of ΔG (Fig. 8).

Assuming that the delayed fluorescence is completely resolved from the prompt fluorescence and that the delayed fluorescence comes from a homogeneous population of reaction centers (see below), the free energies calculated from the initial amplitude of delayed fluorescence are independent of any mechanism proposed to account for the multiexponential decay of the delayed fluorescence. However, the free-energy gap that we have calculated between P* and P^F is probably a maximal value, because the 'initial' form of P^F (P_1^F) is defined operationally by the time resolution of our measurements. The 'prompt' fluorescence from reduced reaction centers could include delayed fluorescence from earlier, unresolved forms of P^F that lie closer to P*. A suggestion that this may be the case comes from the observation that, at room temperature, the apparent amount of prompt fluorescence (α) is about 30% greater than the prompt fluorescence from the unreduced reaction centers (Fig. 3). Possibly, a change in the extent of very rapid, unresolved relaxations of P^F could explain the increase in the initial delayed fluorescence amplitude with decreasing temperature in the region between 200 and 250 K (Fig. 5) and the resulting nonlinearity in ΔG (Fig. 8).

The decay kinetics of the delayed fluorescence

The rate constant determined for the slow component of the delayed fluorescence is similar to the single rate constant found for the decay of the absorbance changes associated with P^F [15]. Its behavior both as a function of temperature and in the presence of a magnetic field are nearly identical to that seen for the P^F absorbance changes. In a multistate system, no single observed rate constant will necessarily be identical to any particular microscopic rate constant, but it seems clear that the slowest component of the delayed fluorescence reflects the overall decay of state P^F.

The nature of the two faster decay components of the delayed fluorescence is less clear. The multiexponential decay kinetics probably do not result simply from heterogeneity in the reaction center preparation, because such heterogeneity presumably would be reflected in the decay kinetics of P^F measured spectrophotometrically. An additional argument that the multiexponential fluorescence decay kinetics are not due to heterogeneity in the preparation is that similar kinetics were obtained with two different preparations of reaction centers. Further, similar kinetic components are seen in the delayed fluorescence from intact chromatophores (Woodbury, N. and Parson, W., unpublished data).

After the submission of this manuscript, Seban and Barbet [45] reported on phase fluorimetry measurements of reduced reaction centers at room temperature. They also found three components in the delayed fluorescence, with time constants of 0.8, 1.5, and 12 ns. The slowest and fastest time constants agree well with those we have determined. The middle component is shorter than our value of 3.2 ns. It is unlikely that this minor difference is due to our use of different bacterial strains, because we have measured a delayed fluorescence component of 3 to 4 ns in chromatophores of *Rhodopseudomonas sphaeroides* strains 2:4:1 and R-26, and of *Rhodospirillum rubrum* G9 and S1 (Woodbury, N. and Parson, W., unpublished data).

The two early components of delayed fluorescence could reflect changes in the excited singlet state P*. It is possible that the excited state formed after charge recombination in P^F has a different energy then the original excited state, if for example, the electron transfer reactions cause movements of the chromophores or neighboring molecules. If the energy of the excited state increases with time, the amount of P* in equilibrium with P^F would decrease, leading to a decrease in the delayed fluorescence. The k_f for P* also could change as a function of time. In either case, a shift in the fluorescence emission spectrum would be expected. In order to change the effective equilibrium constant between P^F and P* by a factor of four (which is the total change between the initial amplitude of the fastest component and that of the slowest component) an energy increase of about 0.036 eV in P* would be required at 295 K. This is equivalent to a spectral shift of about 24 nm. Fig. 6 shows spectra of photons counted between 0 and 2 ns after excitation and between 10 and 38.5 ns. During the first 2 ns, the fluorescence is mostly (at least 80%) prompt fluorescence, which presumably is emitted largely during the initial lifetime of P*. The photons detected between 10 and 38.5 ns are almost exclusively due to the slow component of delayed fluorescence (at least 95%). At 295 K, the spectrum measured at the later time is shifted to longer wavelengths by about 2 nm. This is in the wrong direction to be consistent with an increasing energy of P* with time, and is too small to affect k_f significantly. (The values of k_f calculated from the two spectra differ by less than 10%.) Both emission spectra were measured at seven temperatures from 130 to 295 K, and at no temperature was the difference between their maxima large enough to support either of the mechanisms described above.

If the multiexponential decay does not arise from changes in P*, it probably arises from relaxations in the free energy of P^F. In order to explain three components of delayed fluorescence, a model for P^F including at least three substates is required. Since the electron transfer reaction that creates P^F is very fast on the time scale of the delayed fluorescence [1–7], it seems reasonable to assume that equilibration between P* and one of the substrates (P_1^F) is essentially instantaneous. Fast equilibration between P* and the other two substates of P^F must not occur, since this would eliminate the multiexponential nature of the delayed fluorescence. A general model incorporating these restrictions is given in Scheme I in Fig. 9.

As pointed out above, the rate constant of the slowest component of delayed fluorescence agrees well with the rate constant for decay of the absorption changes associated with P^F. Recent studies with improved time resolution have confirmed that the decay of P^F is well described by a single exponential (Chidsey, C.E.D., Kirmaier, C., Holten, D. and Boxer, S.G., personal communication; and Van Bachove, A.C., Van Grondelle, R., Woodbury, N. and Parson, W.W., unpublished data). The only way to reconcile a mono-exponential decay of P^F with the reaction sequence shown in Scheme I is to assume that the rate constants by which the three substates decay to P^R or the ground state are essentially identical. The overall state P^F then will decay with a single rate constant (k_d) that matches the slowest component of the delayed fluorescence, as is observed.

Seven rate constant are required to describe the reactions shown in Scheme I (Fig. 9). these are k_d, k_{12}, k_{21}, k_{23}, k_{32}, k_{13} and k_{31}, where k_{ij} is the rate constant for the conversion of P_i^F to P_j^F. With the assumptions implicit in Scheme I and using the observed initial amplitudes and kinetics of the delayed fluorescence, it is possible to solve for six of the seven microscopic rate constants, given the

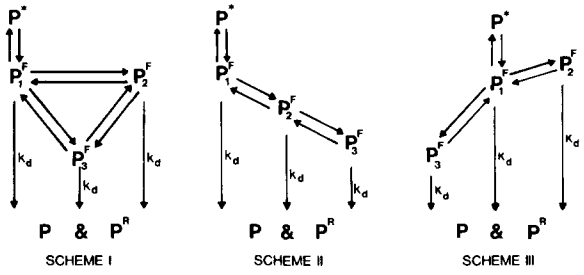

Fig. 9. (Scheme I) General scheme assuming fast equilibrium between P* and P_1^F and a common decay rate (k_d) to P^R and the ground state for each of the substates (P_1^F, P_2^F, and P_3^F). Interconversions between all three substates are allowed. (Scheme II) A simplified scheme assuming a linear relaxation of P^F through P_1^F, P_2^F, and P_3^F. P_3^F cannot be formed directly from P_1^F. (Scheme III) Another simplified scheme assuming P_1^F can relax by equilibration with either of two substates (P_2^F or P_3^F). P_2^F and P_3^F are not directly interconvertable.

seventh. By varying the undetermined rate constant we found that the reaction sequences shown in Schemes II and III (Fig. 9) represent limiting cases (see Appendix). The linear Scheme II is obtained by setting k_{13} and $k_{31} = 0$; the branched Scheme III, by setting k_{23} and $k_{32} = 0$. All the microscopic rate constants vary monotonically between these cases, as do the free-energy differences between the substates. The rate constants and ΔG values for the limiting cases are given in Table III. The maximum ΔG between any two substrates of P^F is in the range between 0.043 and 0.054 eV, depending on the value of the undetermined rate constant. The relaxations thus involve relatively small changes in free energy, compared to the free energy difference of 0.16 eV between P* and P_1^F.

One possible relaxation in P^F is equilibration between the singlet and triplet forms of the radical pair, $^1[P^+I^-]$ and $^3[P^+I^-]$. Because only $^1[P^+I^-]$ can return to P*, the spin rephasing that leads to $^3[P^+I^-]$ would decrease the level of delayed fluorescence. However, weak magnetic fields, which decrease the rate of formation of $^3[P^+I^-]$ by about a factor of 3 [20,22,23,46,47], have no significant effect on the lifetimes of the faster and intermediate components of the delayed fluorescence (Table I and Fig. 4). These components of the relaxation thus appear to be unrelated to spin rephasing.

A second possible relaxation mechanism is equilibration between different charge transfer states, such as P^+BChl^- and P^+BPh^-. An observation that may support this interpretation is that the decay constants of the two faster components of the delayed fluorescence are essentially independent of the temperature (Fig. 4). Electron transfer is one of the few reactions that can be temperature independent. However, in unreduced reaction centers, P^+BChl^- and P^+BPh^- appear to reach equilibrium in about 7 ps [1–7]. The fast and intermediate components of the delayed fluorescence are slower than this by factors of 10^2–10^3. The electron-transfer reactions could be slowed by the reduction of Q [45], but there is no direct evidence for this supposition. The reduction of BPh^- is not slowed significantly when later electron transfer steps are blocked by the extraction of Q [48]. Reduction of the quinone does appear to shift the equilibrium between P^+ $BChl^-$ and P^+ BPh^- in the direction of P^+BChl^- [11], but this is a relatively small effect quantitatively. Absorbance measurements with a time resolution of about 3 ns using reduced reaction centers have not revealed any electron-transfer processes that correlate with the intermediate component of the fluorescence [11].

A third possible mechanism of relaxation is through nuclear movements in the protein, solvent or chromophores [34,45]. Nuclear movements could be driven by coulombic interactions between P^+ and I^-, or by interactions of the protein or solvent with P^+I^-. Several investigators have pointed out that dielectric relaxations may be important in the stabilization of P^+I^- and P^+Q^- [49–52]. Kleinfeld, Okamura and Feher [53] have shown recently that reaction centers that are cooled to 77 K in the state P^+Q^- exhibit different kinetics for the back-reaction between P^+ and Q^- and for the reaction between the primary and secondary quinone, compared to reaction centers that are cooled in the ground state PQ. These observations suggest that the formation of P^+Q^- causes significant conformation changes, which become irreversible at low temperature. Karplus and McCam-

TABLE III

RATE CONSTANTS AND FREE ENERGIES FOR SCHEMES II AND III AT 295 K

The observed time constants and initial amplitudes used for these calculations are given in the first row of Table I.

Scheme	Rate constant (ns^{-1})						Free-energy difference (eV)		
	k_{12}	k_{21}	k_{23}	k_{32}	k_{13}	k_{31}	$P_1^F \rightleftharpoons P_2^F$	$P_2^F \rightleftharpoons P_3^F$	$P_2^F \rightleftharpoons P_3^F$
II	0.878	0.428	0.210	0.080	0	0	−0.018	−0.025	(−0.043) [a]
III	0.536	0.667	0	0	0.359	0.054	+0.006	(−0.054) [a]	−0.048

[a] Calculated from the other free-energy differences using $(k_{12}/k_{21}) \times (k_{23}/k_{32}) = k_{13}/k_{31}$.

mon [54] point out that relaxations of proteins from one thermodynamically distinct conformation to another typically take place on the time scale of 10^{-9}–to 10^{-6} s. The measured relaxations of P^F fall in this time range. However, one would expect nuclear relaxations to decrease in speed at low temperatures. This is difficult to reconcile with the behavior of the delayed fluorescence. The nature of the relaxations thus remains unclear, although nuclear movements appear to us to provide the most likely explanation.

Appendix

The solution to the general three-state first-order system [54] can be extended to the four-state model presented here (P_1^F, P_2^F, P_3^F and the ground state P). Briefly, the rate equations can be expressed as:

$$\frac{d[P_i^F]}{dt} + \sum_{j=1}^{4} K_{ij}[P_j^F] = 0, \quad i = 1,2,3,4$$

$$K_{ij} = -k_{ij}, \quad \text{for } i \neq j$$

$$K_{ii} = \sum_{p=1}^{4} k_{ip}$$

where $[P_i^F]$ is the concentration of the ith state, and k_{ij} is the microscopic rate constant for the transition from state i to state j.

If one assumes the particular solution:

$$[P_i^F] = C_i e^{-kt}$$

one obtains four simultaneous equations:

$$\sum_{j=1}^{4} (K_{ij} - \delta_{ij}k)C_j = 0, \quad i = 1,2,3,4 \qquad \text{(A-1)}$$

For a nontrivial solution:

$$|K_{ij} - \delta_{ij}k| = 0$$

This gives a cubic equation with three nontrivial solutions for k (k_r with $r = 1, 2, 3$) in terms of the rate constants k_{ij}, and one trivial solution, $k_4 = 0$. In practice the cubic equation does not have to be solved explicitly. Instead the determinant is expanded and the coefficients are equated to the appropriate coefficients of the expression:

$$(k - k_1)(k - k_2)(k - k_3) = 0$$

or:

$$k^3 - (k_1 + k_2 + k_3)k^2 + (k_1k_2 + k_2k_3 + k_1k_3)k - k_1k_2k_3 = 0$$

giving three relations between k_1, k_2, k_3 and the microscopic rate constants. Each k_r is associated with a set of four coefficients, C_{jr} with $j = 1, 2, 3, 4$. One of the coefficients can be chosen arbitrarily, and the other three obtained relative to this one with Eqn. A-1. In general, the desired solution will be some combination of particular solutions:

$$[P_j^F] = \sum_{r=1}^{4} C_{jr}B_r e^{-k_r t} \qquad \text{(A-2)}$$

where B_r is defined by the initial conditions. We assume that P_1^F is formed instantaneously with 100% quantum yield. Thus at $t = 0$, $[P_1^F] = 1$ and $[P_j^F] = 0$ for $j = 2, 3, 4$. Since delayed fluorescence originates from P*, and P* is in fast equilibrium with P_1^F (but not P_2^F or P_3^F), the amplitude of the delayed fluorescence at any time is proportional to $[P_1^F]$. Setting $C_{1r} = 1$ gives:

$$[P_1^F] = \sum_{r=1}^{4} B_r e^{-k_r t} \qquad \text{(A-3)}$$

We equate the coefficients in this expression (B_r) to the measured initial amplitudes of the delayed fluorescence components, and equate the k_r to the observed decay rate constants.

In Schemes I–III in Fig. 9, $B_4 = 0$ because back reactions from the ground state and P^R to P^F and P* are taken to be negligible. Relating k_1, k_2 and k_3 to the microscopic rate constants k_{ij}, and relating B_r to C_{jr}, k_r and k_{ij} using Eqns. A-2 and A-1 as well as the initial conditions described above, we have five independent equations and seven variables (the measured amplitudes are relative, which adds one degree of freedom). Noting also that $(k_{12}/k_{21}) \times (k_{23}/k_{32}) = (k_{13}/k_{31})$, six of the seven rate constants can be determined, given the 7th. In practice, a successive approximation algorithm was used to solve the equations numerically

for k_{12}, k_{21}, k_{23}, k_{32} and k_{13}/k_{31}. The sum $k_{13} + k_{31}$ was varied over the physically meaningful range (k_{13} and $k_{31} \geq 0$). Setting $k_{13} + k_{31} = 0$ gives scheme II (Fig. 9). Increasing this sum causes a monotonic variation in each of the other parameters. As $k_{13} + k_{31}$ approaches 0.41 ns^{-1}, k_{23} and k_{32} both approach zero, which results in scheme III (Fig. 9). For $k_{13} + k_{31}$ greater than 0.41 ns^{-1} but less than 1.20 ns^{-1}, one or more of the calculated rate constants is negative. When $k_{13} + k_{31}$ approaches 1.20 ns^{-1}, k_{23} and k_{32} again approach zero, giving scheme III with states P_2^F and P_3^F reversed. As $k_{13} + k_{31}$ is increased further to 1.32 ns^{-1}, the reaction sequence shown in scheme II is obtained except that P_2^F and P_3^F are reversed. At higher values of $k_{13} + k_{31}$, k_{12} and k_{21} become negative. Thus shcemes II and III represent the limiting cases which bound the range of microscopic rate constants and energy differences consistent with the delayed fluorescence measurements and Scheme I.

Acknowledgments

We thank Drs. E. Schlodder, R. van Grondelle, J. Thomas and J. Shibata for assistance in developing the experimental protocol and for helpful discussions, Drs. G. Feher, D. Kleinfeld, S. Boxer and D. Holten for access to unpublished manuscripts, and J. Rutberg and M. Remeroski for preparation of reaction centers. This work was supported by NSF grant PCM 8016593. N. Woodbury was supported in part by Public Health Service National Research Service Award GM 07270 from the National Institutes of Health.

References

1 Zankel, K.L., Reed, D. Wo and Clayton, R.K. (1968) Proc. Natl. Acad. Sci. USA 61, 1243–1249
2 Rockley, M.G., Windsor, M.W., Cogdell, R.J. and Parson, W.W. (1975) Proc. Natl. Acad. Sci. USA 72, 2251–2255
3 Kaufmann, K.J., Dutton, P.L., Netzel, T.L., Leigh, H.S. and Rentzepis, P.M. (1975) Science 188, 1301–1304
4 Holten, D., Hoganson, C., Windsor, M.W., Schenck, C.C., Parson, W.W., Migus, A., Fork, R.L. and Shank, C.V. (1980) Biochim. Biophys. Acta 592, 461–467
5 Shuvalov, V.A., Klevanik, A.V., Sharkov, A.V., Matveetz, Yu.A. and Krukov, P.G. (1978) FEBS Lett. 91, 135–139
6 Paschenko, V.S., Kononenko, A.A., Protasov, S.P., Rubin, A.B., Rubin, L.B. and Uspenskaya, N.Ya. (1977) Biochim. Biophys. Acta 461, 403–412
7 Kononenko, A.A., Knox, P.P., Adamova, N.P., Paschenko, V.Z., Timofeev, K.N. and Rubin, A.B. (1976) Studia Biophys. 55, 183–198
8 Holten, D., Windsor, M.W., Parson, W.W. and Thornber, J.P. (1978) Biochim. Biophys. Acta 501, 112–126
9 Shuvalov, V.A. and Klimov, V.V. (1976) Biochim. Biophys. Acta 440, 587–599
10 Dutton, P.L., Prince, R.C., Tiede, D.M., Petty, K.M., Kaufmann, K.J., Netzel, T.L. and Rentzepis, P.M. (1977) Brookhaven Symp. Biol. 28, 213–237
11 Shuvalov, V.A. and Parson, W.W. (1981) Proc. Natl. Acad. Sci. USA 78, 957–961
12 Dutton, P.L., Leigh, J.S. and Seibert, M. (1972) Biochem. Biophys. Res. Commun. 46, 406–413
13 Parson, W.W., Clayton, R.K. and Cogdell, R.J. (1975) Biochim. Biophys. acta 387, 265–278
14 Cogdell, R.J., Monger, T.G. and Parson, W.W. (1975) Biochim. Biophys. Acta 408, 189–199
15 Schenck, C.C., Blankenship, R.E. and Parson, W.W. (1982) Biochim. Biophys. Acta 680, 44–59
16 Van Grondelle, R., Holmes, N.G., Rademaker, H. and Duysens, L.N.M. (1978) Biochim. Biophys. Acta 503, 10–25
17 Godik, V.I. and Borisov, A.Y. (1980) Biochim. Biophys. Acta 548, 296–308
18 Godik, V.I. and Borisov, A.Y. (1980) Biochim. Biophys. Acta 590, 182–193
19 Norris, J.R., Bowman, M.K., Budil, D.E., Tang, J. Wraight, C.A. and Closs, G.L. (1982) Proc. Natl. Acad. Sci. USA 79, 5532–5536
20 Tang, J. and Norris, J.R. (1982) Chem. Phys. Lett. 92, 136–140
21 Holmes, N.G., Van Grondelle, R., Hoff, A.J. and Duysens, L.N.M. (1976) FEBS Lett. 70, 185–190
22 Roelofs, M.G., Chidsey, C.E.D. and Boxer S.G. (1982) Chem. Phys. Lett. 87, 582–588
23 Ogrodnik, A., Kruger, H.W., Orthuber, H., Haberkorn, R., Michel-Beyerle, M.E. and Scheer, H. (1982) Biophys. J. 39, 91–100
24 Rademaker, J. and Hoff, A.J. (1981) Biophys. J. 34, 325–344
25 Godik, V.I., Kotova, E.A. and Borisov, A.Yu. (1982) Photochem. and Photophys. 4, 219–226
26 Sebban, P. and Moya, I. (1983) Biochim. Biophys. Acta 722, 436–442
27 Van Bochoven, A.C., Van Grondelle, R. and Duysens, L.N.M. (1981) in Photosynthesis (Akoyunoglou, G., ed.), pp. 989–996, Balaban International Science Services, Philadelphia, PA
28 Rademaker, H. and Hoff, A.J., and Duysens, L.M.N. (1979) Biochim. Biophys. Acta 546, 248–255
29 Voznyak, V.M., Elfimov, E.I. and Sukovatitzina, V.K. (1980) Biochim. Biophys. Acta 592, 235–239
30 Carithers, R.P. and Parson, W.W. (1975) Biochim. Biophys. Acta 387, 194–211
31 Clayton, R.K. (1965) J. Gen. Physiol. 48, 633–646
32 Zankel, K.L. (1969) Photochem. Photobiol. 10, 259–266
33 Clayton, R.K. (1977) in Photosynthetic Organelles. Structure and Function (Miyachi, S., Katoh, S., Fujita, Y. and Shibata, K., eds.), special issue of Plant Cell Physiol., pp. 87–96

34 Parson, W., Holten, D., Kirmaier, C., Scherz, A. and Woodbury, N. (1984) in Advances in Photosynthesis Research (Sybesma, C., ed.), Vol. I, pp. 187–194, Martinus Nijhoff/Dr. W. Junk Publishers, The Hague
35 Satir, R., Schneider, W.E. and Jackson, J.K. (1963) Applied Optics 2, 1151–1154
36 Thomas, J.C., Allison, S.A., Appellof, C.J. and Schurr, M.J. (1980) Biophys. Chem. 12, 177–188
37 Grinvald, A. and Steinberg, I.Z. (1974) Anal. Biochem. 59, 583–598
38 Grinvald, A. (1976) Anal. Biochem. 75, 260–280
39 Slooten, L. (1973) Ph.D. Thesis, State University, Leiden, The Netherlands
40 Arata, H. and Parson, W.W. (1981) Biochim. Biophys. Acta 638, 201–209
41 Strickler, S.J. and Berg, R.A. (1962) J. Chem. Phys. 37, 814–822
42 Ross, R.T. (1975) Photochem. Photobiol. 21, 401–406
43 Arata, H. and Nishimura, M. (1983) Biochim. Biophys. Acta 725, 394–401
44 Clayton, R.K. and Yau, H.F. (1972) Biophys. J. 12, 867–881
45 Seban, P. and Barbet, J.C. (1984) FEBS Lett. 165, 107–110
46 Hoff, A., J., Rademaker, H., Van Grondelle, R. and Duysens, L.N.M. (1977) Biochim. Biophys. Acta 460, 547–554
47 Haberkorn, R. and Michel-Beyerle, M.E. (1979) Biophys. J. 26, 489–498
48 Kaufmann, K.J., Petty, K.M., Dutton, P.L. and Rentzepis, P.M. (1976) Biochem. Biophys. Res. Commun. 70, 839–845
49 Parak, F., Frolov, E.N., Kononenko, A.A., Mossbauer, R.L. and Goldansky, V.I. (1980) FEBS Lett. 117, 368–372
50 Rubin, A.B., Kononenko, A.A., Venediktov, P.S., Borisevich, G.P., Knox, P.P. and Lukashev, E.P. (1980) Int. J. Quantum. Chem. 17, 587–593
51 Kleinfeld, D., Okamura, M.Y. and Feher, G. (1983) Biophys. J. 41, 121a
52 Warshel, A. (1980) Proc. Natl. Acad. Sci. USA 77, 3105–3109
53 Kleinfeld, D., Okamura, M.Y. and Feher, G. (1984) Biochim. Biophys. Acta 766, 126–140
54 Karplus, M. and McCammon, J.A. (1981) CRC Crit. Rev. Biochem. 9, 293–349
55 Frost, A.A. and Pearson, R.G. (1952) Kinetics and Mechanism, pp. 232–245, John Willey and Sons, London
56 Reed, D.W. and Ke, B. (1973) J. Biol. Chem. 248, 3041–3045
57 Feher, G. and Okamura, M.Y. (1976) Brookhaven Symposia in Biology 28, 183–194